Hindawi
Advances in Mathematical Physics
Volume 2019, Article ID 7296461, 15 pages
https://doi.org/10.1155/2019/7296461

Research Article

Dynamic Study of a Predator-Prey Model with Weak Allee Effect and Delay

Yong Ye,[1] **Hua Liu**,[1] **Yu-mei Wei**,[2] **Ming Ma**,[1] **and Kai Zhang**[1]

[1] *School of Mathematics and Computer Science, Northwest Minzu University, Lanzhou 730000, China*
[2] *Experimental Center, Northwest Minzu University, Lanzhou 730000, China*

Correspondence should be addressed to Hua Liu; 7783360@qq.com

Received 12 June 2019; Accepted 22 July 2019; Published 6 August 2019

Academic Editor: Ming Mei

In this paper, a prey-predator model and weak Allee effect in prey growth and its dynamical behaviors are studied in detail. The existence, boundedness, and stability of the equilibria of the model are qualitatively discussed. Bifurcation analysis is also taken into account. After incorporating the searching delay and digestion delay, we establish a delayed predator-prey system with Allee effect. The results show that there exist stability switches and Hopf bifurcation occurs while the delay crosses a set of critical values. Finally, we present some numerical simulations to illustrate our theoretical analysis.

1. Introduction

Some researchers have conducted extensive research on the dynamics of interacting prey-predator models to understand the long-term behavior of species. A wide variety of nonlinear coupled ordinary differential equation models are proposed and analyzed for the interaction between prey and their predators. The classic predator-prey model is the Lotka-Volterra model, which was independently proposed by Lotka in the United States in 1925 and Volterra in Italy in 1926 [1, 2]. The model was developed on the basis of a single-population growth model and has wide applicability. The mathematical form of the Lotka-Volterra model is

$$\begin{aligned} \frac{dx}{dt} &= rx - axy \\ \frac{dy}{dt} &= cxy - my \end{aligned} \tag{1}$$

In population dynamics,when the population density is very low, there is a positive correlation between the population unit growth rate and the population density. This phenomenon can be called the Allee effect [3–5], starting with Allee's research [6]. The Allee effect is classified according to the density-dependent properties at low density. If the population density is low, a strong Allee effect will appear. If the proliferation rate is positive and increases, the Allee effect will be weak. Demographic Allee effects can be either weak or strong [7, 8]. When the density is below the critical threshold, the population affected by the strong Allee effect will have a negative average growth rate. Under deterministic dynamics, we find that populations that do not exceed this threshold will be extinct. Many jobs only consider the strong Allee effect, but in the work of Allee it is clear that the Allee effect also has a weak Allee effect [8–13].

Today, it is widely believed that the Allee effect greatly increases the likelihood of local and global extinction and can produce a rich variety of dynamic effects [14–16]. And it is interesting and important to study the impact of Allee effect on the predator-prey models [17–19]. In this paper, we introduced a predator-prey model with weak Allee effect:

$$\begin{aligned} \frac{dx}{dt} &= rx\left(1 - \frac{x}{K}\right)\frac{x}{x+A} - axy \\ \frac{dy}{dt} &= c(ax)y - my \\ x(0) &\geq 0 \\ y(0) &\geq 0 \end{aligned} \tag{2}$$

Here, the weak Allee effect term is $P(x) = x/(x + A)$, where $A > 0$ is described as a "weak Allee effect constant" ([12]). x is the prey population and y is the predator population, m is the intrinsic death rate of predators, c is the conversion efficiency from prey to predator, K is the carrying capacity, r is the intrinsic growth rate of prey, and a is the prey capture rate by their predators. It is more realistic to introduce time delay on the basis of traditional predator-prey model because it exists almost everywhere in biological activities and is considered as one of the reasons for the regular change of population density [20–26]. Therefore, in order to make the system established in this paper biologically closer to reality, incorporating the searching delay and digestion delay in the system (2) is interesting. Based on the above considerations, We establish a predator-prey model with time delay and weak Allee effect, as follows:

$$\begin{aligned}\frac{dx(t)}{dt} &= rx(t)\left(1-\frac{x(t)}{K}\right)\frac{x(t)}{x+A} \\ &\quad - ax(t-\tau_1)\,y(t-\tau_1) \\ \frac{dy(t)}{dt} &= c\left(ax(t-\tau_2)\right)y(t-\tau_2) - my(t) \\ x(0) &\geq 0 \\ y(0) &\geq 0\end{aligned} \tag{3}$$

where the time delay τ_i $(i = 1, 2)$ is the controlling or perturbed parameters, τ_1 is the searching delay, and τ_2 is the digestion delay.

The latter parts of the paper are described as follows. In Section 2, we discuss the boundedness, the stability of the equilibria, and bifurcation of the model (2) in detail. In Section 3, we investigated local stability property of interior equilibrium point of the model (3) with time delay; the Hopf bifurcation around the positive equilibrium point is also studied. In Section 4, we verify the previous theoretical derivation by numerical simulation.

2. A Predator-Prey Model with Weak Allee Effect

We easily see that model (2) exhibits three equilibrium points $E_0 = (0, 0)$, $E_1 = (K, 0)$, and $E_* = (x_*, y_*)$. Here $x_* = m/ca$, $y_* = (Krx_* - rx_*^{\,2})/aK(x_* + A)$. And for the positive equilibrium point(s), we have $m/ca < K$.

2.1. Boundedness

Theorem 1. *For the solution $(x(t), y(t))$ of model,*

$$\limsup_{t\to\infty}\left(x(t)+\frac{1}{c}y(t)\right) \leq \frac{K(m+r)^2}{4rm}. \tag{4}$$

Proof. We define $\chi = x(t) + (1/c)y(t)$. Then we can easily see that along the solution of system (2),

$$\begin{aligned}\frac{d\chi}{dt} &= \frac{dx}{dt} + \frac{1}{c}\frac{dy}{dt} \\ &= rx\left(1-\frac{x}{K}\right)\frac{x}{x+A} - axy + \frac{1}{c}c(ax)y - \frac{1}{c}my \\ &= rx\left(1-\frac{x}{K}\right)\frac{x}{x+A} - \frac{m}{c}y.\end{aligned} \tag{5}$$

Thus, we see that for all large $t > 0$

$$\begin{aligned}\frac{d\chi}{dt} + m\chi &= rx\left(1-\frac{x}{K}\right)\frac{x}{x+A} - \frac{m}{c}y + mx + m\frac{1}{c}y \\ &= rx\left(1-\frac{x}{K}\right)\frac{x}{x+A} + mx \\ &\leq rx\left(1-\frac{x}{K}\right) + mx = x\left(r+m-\frac{r}{K}x\right) \\ &\leq \frac{K}{4r}(m+r)^2.\end{aligned} \tag{6}$$

Hence the standard comparison argument shows that

$$\limsup_{t\to\infty}\left(x(t)+\frac{1}{c}y(t)\right) \leq \frac{K(m+r)^2}{4rm}. \tag{7}$$

□

2.2. Stability Analysis

Theorem 2. *(1) Trivial equilibrium point E_0 is always a saddle-node point.*

(2) E_1 is stable for $a < m/cK$ and is a saddle point otherwise.

(3) Coexistence equilibrium E_* is locally asymptotically stable for $A < x_*^{\,2}/(K - 2x_*)$ and is unstable node otherwise.

Proof. Let

$$\begin{aligned}f(x,y) &= rx\left(1-\frac{x}{K}\right)\frac{x}{x+A} - axy \\ g(x,y) &= c(ax)y - my.\end{aligned} \tag{8}$$

So, the Jacobian matrix for the model (2) is given by $J = \begin{pmatrix} \partial f/\partial x & \partial f/\partial y \\ \partial g/\partial x & \partial g/\partial y \end{pmatrix}$ where

$$\begin{aligned}\frac{\partial f}{\partial x} &= \frac{-2rKx^3 + rKx^2 - 3rAx^2 + 2rAKx}{K(x+A)^2} - ay, \\ \frac{\partial f}{\partial y} &= -ax, \\ \frac{\partial g}{\partial x} &= cay, \\ \frac{\partial g}{\partial y} &= cax - m.\end{aligned} \tag{9}$$

So we get

$$J = \begin{pmatrix} \dfrac{-2rx^3 + rKx^2 - 3rAx^2 + 2rAKx}{K(x+A)^2} - ay & -ax \\ cay & cax - m \end{pmatrix}. \quad (10)$$

First, it can be concluded by calculating the Jacobian matrix of the model (2) at E_0 given by

$$J_0 = \begin{pmatrix} 0 & 0 \\ 0 & -m \end{pmatrix}. \quad (11)$$

And hence E_0 is always a saddle-node point. Then, by evaluating the Jacobian matrix of the model (2) at E_1, we find

$$J_1 = \begin{pmatrix} \dfrac{-rK}{K+A} & -aK \\ 0 & caK - m \end{pmatrix}. \quad (12)$$

First eigenvalue $-rK/(K+A)$ is negative; hence E_1 is stable if $caK - m < 0$ implying $a < m/cK$, and E_1 is a saddle point when $a > m/cK$. Finally, the Jacobian matrix for the model (2) evaluated at E_* is given by

$$J_* = \begin{pmatrix} \dfrac{-2rx_*{}^3 + rKx_*{}^2 - 3rAx_*{}^2 + 2rAKx_*}{K(x_*+A)^2} - ay_* & -\dfrac{m}{c} \\ cay_* & 0 \end{pmatrix}. \quad (13)$$

The characteristic polynomial is

$$H(\lambda) = \lambda^2 - T\lambda + D \quad (14)$$

where $T = -rx_*(x_*{}^2 + 2Ax_* - AK)/K(x_*+A)^2$ and $D = may_*$. Thus, we have the following conclusions. (1) If $T < 0$ and $A < x_*{}^2/(K - 2x_*)$, then the positive equilibrium is locally asymptotically stable. (2) If $T > 0$ and $A > x_*{}^2/(K - 2x_*)$, then the positive equilibrium is unstable. □

Theorem 3. $E_1 = (K, 0)$ *is globally stable when* $a < m/cK$.

Proof. Consider the Lyapunov function:

$$V(x,y) = \int_K^x \frac{u-K}{u}\,du + \frac{1}{c}y. \quad (15)$$

The derivative of V along the solution of the model is

$$\begin{aligned} \dot{V} &= \frac{x-K}{x}\frac{dx}{dt} + \frac{1}{c}\frac{dy}{dt} \\ &= \frac{x-K}{x}\left[rx\left(1-\frac{x}{K}\right)\frac{x}{x+A} - axy\right] \\ &\quad + \frac{1}{c}\left[c(ax)y - my\right] \\ &= (x-K)\left[r\left(1-\frac{x}{K}\right)\frac{x}{x+A}\right] - a(x-K)y + axy \\ &\quad - \frac{m}{c}y \\ &= (x-K)\frac{rKx - rx^2}{K(x+A)} - a(x-K)y + axy - \frac{m}{c}y \\ &= \frac{-rx(x-K)^2}{K(x+A)} + aKy - \frac{m}{c}y \le aKy - \frac{m}{c}y. \end{aligned} \quad (16)$$

□

2.3. Bifurcation Analysis

2.3.1. Transcritical Bifurcation

Theorem 4. *The model enters into transcritical bifurcation around* E_1 *at* $a = a_0$*, where* $a_0 = m/cK$.

Proof. One of the eigenvalues of J_1 will be zero if $J_1 = 0$ which gives $a = a_0$. At this point, the other eigenvalue is $-rK/(K+A)$. If V and W denote the eigenvectors corresponding to the eigenvalue 0 of the matrices J_1 and $J_1{}^T$, respectively, then we obtain $V = (-a(K+A)/r, 1)^T$ and $W = (0,1)^T$, where $J_1{}^T = \begin{pmatrix} -rK/(K+A) & 0 \\ -aK & 0 \end{pmatrix}$, $V_1 = -a(K+A)/r$, $V_2 = 1$.

$$\begin{aligned} & W^T f_a(\overline{x}, \overline{y}, a_0) = 0, \\ & W^T\left[Df_a(\overline{x}, \overline{y}, a_0)V\right] = cK \ne 0, \\ & W^T\left[D^2 f(\overline{x}, \overline{y}, a_0)(V,V)\right] \\ &= W^T \begin{pmatrix} \dfrac{\partial^2 f_1}{\partial x^2}V_1{}^2 + 2\dfrac{\partial^2 f_1}{\partial x \partial y}V_1V_2 + \dfrac{\partial^2 f_1}{\partial y^2}V_2{}^2 \\ \dfrac{\partial^2 f_2}{\partial x^2}V_1{}^2 + 2\dfrac{\partial^2 f_2}{\partial x \partial y}V_1V_2 + \dfrac{\partial^2 f_2}{\partial y^2}V_2{}^2 \end{pmatrix}_{(\overline{x}, \overline{y}, a_0)} \\ &= \frac{-2a^2(K+A)}{r} \ne 0. \end{aligned} \quad (17)$$

Therefore, by the Sotomayor theorem, we can find that the model experiences transcritical bifurcation at $a = a_0$ around the axial equilibrium E_1. □

2.3.2. Hopf Bifurcation. From Theorem 2, model (2) undergoes bifurcation if $A = {x_*}^2/(K - 2x_*)$. The purpose of this section is to show that model (2) undergoes a Hopf bifurcation if $A = {x_*}^2/(K - 2x_*)$. We analyze the Hopf bifurcation occurring at $E_* = (x_*, y_*)$ by choosing as the bifurcation parameter. Denote

$$A_0 = \frac{{x_*}^2}{K - 2x_*}. \tag{18}$$

When $A = A_0$, we have $T = -rx_*({x_*}^2 + 2Ax_* - AK)/K(x_* + A)^2 = 0$. Thus, the Jacobian matrix J_* has a pair of imaginary eigenvalues $\lambda = \pm i\sqrt{may_*}$. Let $\lambda = \alpha(A) \pm \beta(A)i$ be the roots of $\lambda^2 - T\lambda + D = 0$; then

$$\begin{gathered}\alpha^2 - \beta^2 - \alpha T + D = 0\\ 2\alpha\beta - T\beta = 0\end{gathered} \tag{19}$$

and

$$\begin{gathered}\alpha = \frac{T}{2}\\ \beta = \frac{\sqrt{4D - T^2}}{2}\\ \left.\frac{d\alpha}{dA}\right|_{A=A_0} = \frac{-r{x_*}^3}{2AK\left(x_* + A\right)^2} < 0\end{gathered} \tag{20}$$

By the Poincare-Andronov-Hopf Bifurcation Theorem, we know that model (2) undergoes a Hopf bifurcation at $E_* = (x_*, y_*)$ when $A = A_0$. However, the detailed nature of the Hopf Bifurcation needs further analysis of the normal form of the model. Set $x = X + x_*$ and $y = Y + y_*$, to (x_*, y_*) as origin of coordinates (X, Y). We have the following model:

$$\begin{aligned}\frac{dX}{dt} &= a_{11}X + a_{12}Y + F_1(X, Y)\\ \frac{dY}{dt} &= a_{21}X + a_{22}Y + F_2(X, Y)\end{aligned} \tag{21}$$

where $a_{11} = (-2r{x_*}^3 + rK{x_*}^2 - 3rA{x_*}^2 + 2rAKx_*)/K(x_* + A)^2 - ay_*$, $a_{12} = -m/c$, $a_{21} = cay_*$, $a_{22} = 0$, and

$$\begin{aligned}&F_1(X, Y)\\ &\quad = A_1X^2 + A_2XY + A_3Y^2 + B_1X^3 + B_2X^2Y + B_3XY^2\\ &\qquad + B_4Y^3 + P_1(X, Y)\\ &F_2(X, Y)\\ &\quad = C_1X^2 + C_2XY + C_3Y^2 + D_1X^3 + D_2X^2Y + D_3XY^2\\ &\qquad + D_4Y^3 + P_2(X, Y)\\ &A_1 = \frac{-r{x_*}^3 - 3rA{x_*}^2 - 3rA^2x_* + rA^2K}{K\left(x_* + A\right)^3},\\ &A_2 = -\frac{a}{2},\\ &A_3 = 0\\ &B_1\\ &\quad = \frac{r{x_*}^3 + (3rA - r){x_*}^2 + \left(3rA^2 - 2rA\right)x_* - \left(rA^2 + rA^2K\right)}{2K\left(x_* + A\right)^3},\\ &B_2 = 0,\\ &B_3 = 0,\\ &B_4 = 0\\ &C_1 = 0,\\ &C_2 = \frac{ca}{2},\\ &C_3 = 0\\ &D_1 = 0,\\ &D_2 = 0,\\ &D_3 = 0,\\ &D_4 = 0\end{aligned} \tag{22}$$

where $P_1(X, Y)$ and $P_2(X, Y)$ are smooth functions of X and Y at least of order four. Now, using the transformation$u = X$, $v = -(1/\beta)(a_{11}X + a_{12}Y)$, we obtain

$$\begin{aligned}\frac{du}{dt} &= -\beta v + G_1(u, v)\\ \frac{dv}{dt} &= \beta u + G_2(u, v)\end{aligned} \tag{23}$$

where

$$\begin{aligned}G_1(u, v) &= F_1\left(u, -\frac{1}{a_{12}}\left(a_{11}u + \beta v\right)\right)\\ G_2(u, v) &= -\frac{1}{\beta}\left(a_{11}F_1\left(u, -\frac{1}{a_{12}}\left(a_{11}u + \beta v\right)\right)\right.\\ &\quad \left.+ a_{12}F_2\left(u, -\frac{1}{a_{12}}\left(a_{11}u + \beta v\right)\right)\right)\end{aligned} \tag{24}$$

so

$$\begin{aligned}G_1(u, v) &= A_1u^2 + A_2u\left(-\frac{1}{a_{12}}\left(a_{11}u + \beta v\right)\right) + B_1u^3\\ G_2(u, v) &= -\frac{1}{\beta}\left[a_{11}\left(A_1u^2\right.\right.\\ &\quad \left.\left.+ A_2u\left(-\frac{1}{a_{12}}\left(a_{11}u + \beta v\right)\right) + B_1u^3\right)\right]\\ &\quad + a_{12}uC_2\left(-\frac{1}{a_{12}}\left(a_{11}u + \beta v\right)\right)\end{aligned} \tag{25}$$

Set

$$\sigma = \frac{1}{16}\left[\frac{\partial^3 G_1}{\partial u^3} + \frac{\partial^3 G_1}{\partial u \partial v^2} + \frac{\partial^3 G_2}{\partial u^2 \partial v} + \frac{\partial^3 G_2}{\partial v^3}\right] + \frac{1}{16\beta}\left[\frac{\partial^2 G_1}{\partial u \partial v}\left(\frac{\partial^2 G_1}{\partial u^2} + \frac{\partial^2 G_1}{\partial v^2}\right) - \frac{\partial^2 G_2}{\partial u \partial v}\left(\frac{\partial^2 G_2}{\partial u^2} + \frac{\partial^2 G_2}{\partial v^2}\right) - \frac{\partial^2 G_1}{\partial u^2}\frac{\partial^2 G_2}{\partial u^2} + \frac{\partial^2 G_1}{\partial v^2}\frac{\partial^2 G_2}{\partial v^2}\right] \quad (26)$$

where

$$\begin{aligned}
\frac{\partial^3 G_1}{\partial u^3} &= 6B_1, \\
\frac{\partial^3 G_1}{\partial u \partial v^2} &= 0, \\
\frac{\partial^3 G_2}{\partial u^2 \partial v} &= 0, \\
\frac{\partial^3 G_2}{\partial v^3} &= 0, \\
\frac{\partial^2 G_1}{\partial u \partial v} &= \frac{A_2 \beta}{a_{12}}, \\
\frac{\partial^2 G_2}{\partial u \partial v} &= \frac{A_2 a_{11}}{a_{12}}, \\
\frac{\partial^2 G_1}{\partial v^2} &= 0, \\
\frac{\partial^2 G_2}{\partial v^2} &= 0, \\
\frac{\partial^2 G_1}{\partial u^2} &= 2\left(A_1 - \frac{A_2 a_{11}}{a_{12}}\right) + 6B_1 u, \\
\frac{\partial^2 G_2}{\partial u^2} &= 2\left(\frac{A_2 a_{11}{}^2}{\beta a_{12}} - \frac{A_1 a_{11}}{\beta}\right) - \frac{6B_1 a_{11}}{\beta} u.
\end{aligned} \quad (27)$$

So

$$\begin{aligned}
\sigma = {} & \frac{3B_1}{8} + \frac{1}{16\beta}\left(\frac{A_2\beta}{a_{12}}\left(2\left(A_1 - \frac{A_2 a_{11}}{a_{12}}\right) + 6B_1 u\right)\right. \\
& - \frac{A_2 a_{11}}{a_{12}}\left(2\left(\frac{A_2 a_{11}{}^2}{\beta a_{12}} - \frac{A_1 a_{11}}{\beta}\right) - \frac{6B_1 a_{11}}{\beta} u\right) \\
& - \left(2\left(A_1 - \frac{A_2 a_{11}}{a_{12}}\right) + 6B_1 u\right) \\
& \left.\cdot\left(2\left(\frac{A_2 a_{11}{}^2}{\beta a_{12}} - \frac{A_1 a_{11}}{\beta}\right) - \frac{6B_1 a_{11}}{\beta} u\right)\right)
\end{aligned} \quad (28)$$

If $\sigma < 0$, the equilibrium E_* is destabilized through a Hopf bifurcation that is supercritical and Hopf bifurcation is subcritical otherwise.

3. Delayed Model with Weak Allee Effect

Let $X(t) = x(t) - x_*$, $Y(t) = y(t) - y_*$; then the model (3) can be expressed as in the following matrix form after linearization:

$$\begin{aligned}
\frac{d}{dt}\begin{pmatrix} X(t) \\ Y(t) \end{pmatrix} &= A_1 \begin{pmatrix} X(t) \\ Y(t) \end{pmatrix} + A_2 \begin{pmatrix} X(t-\tau_1) \\ Y(t-\tau_1) \end{pmatrix} + A_3 \begin{pmatrix} X(t-\tau_2) \\ Y(t-\tau_2) \end{pmatrix}, \\
A_1 &= \begin{pmatrix} \dfrac{-2rx_*{}^3 + rKx_*{}^2 - 3rAx_*{}^2 + 2rAKx_*}{K(x_*+A)^2} & 0 \\ 0 & -m \end{pmatrix}, \\
A_2 &= \begin{pmatrix} -ay_* & -ax_* \\ 0 & 0 \end{pmatrix}, \\
A_3 &= \begin{pmatrix} 0 & 0 \\ cay_* & cax_* \end{pmatrix}.
\end{aligned} \quad (29)$$

3.1. Stability Analysis. The characteristic polynomial is

$$H(\lambda) = \lambda^2 - T\lambda + D \quad (30)$$

where

$$\begin{aligned}
T = {} & \frac{-2rx_*{}^3 + rKx_*{}^2 - 3rAx_*{}^2 + 2rAKx_*}{K(x_*+A)^2} - ay_* e^{-\lambda\tau_1} + cax_* e^{-\lambda\tau_2} - m, \\
D = {} & \left(\frac{-2rx_*{}^3 + rKx_*{}^2 - 3rAx_*{}^2 + 2rAKx_*}{K(x_*+A)^2} - ay_* e^{-\lambda\tau_1}\right)\left(cax_* e^{-\lambda\tau_2} - m\right) + ca^2 x_* y_* e^{-\lambda\tau_1} e^{-\lambda\tau_2}.
\end{aligned} \quad (31)$$

Let

$$G = \frac{\left(-2rx_*{}^3 + rKx_*{}^2 - 3rAx_*{}^2 + 2rAKx_*\right)}{K(x_*+A)^2} \quad (32)$$

So

$$\begin{aligned}
H(\lambda) = {} & \lambda^2 - \left(G - ay_* e^{-\lambda\tau_1} + cax_* e^{-\lambda\tau_2} - m\right)\lambda \\
& - mG + may_* e^{-\lambda\tau_1} + cax_* e^{-\lambda\tau_2} G
\end{aligned} \quad (33)$$

Let $\lambda(\tau) = \eta(\tau) + i\omega(\tau)$, $\eta(\tau_0) = 0$, and $\omega(\tau_0) = \omega_0$.

Theorem 5. *Assume $A < x_*{}^2/(K - 2x_*)$, when $\tau_1 > 0, \tau_2 = 0$; we have the following conclusions. (1) When $4FG - 2Fm + G^2 +$*

$F^2+m^2-D^2>0$ and $-2FmG^2+F^2G^2+m^2G^2-E^2>0$, the positive equilibrium $E_*=(x_*,y_*)$ is locally asymptotically stable. (2) Hopf bifurcation occurs when τ_1 passes the critical value

$$\overline{\tau}_1=\frac{1}{\omega_0}\cdot\arccos\frac{EGm-EFG-\omega_0{}^2mD+\omega_0{}^2FD+\omega_0{}^2GD+\omega_0{}^2E}{\omega_0{}^2D^2+E^2}. \tag{34}$$

Proof. The characteristic equation is

$$\lambda^2-\left(G-ay_*e^{-\lambda\tau_1}+cax_*-m\right)\lambda-mG+may_*e^{-\lambda\tau_1}+cax_*G=0. \tag{35}$$

Next we suppose that $\lambda(\tau_0)=i\omega_0$ is a solution of $H(\lambda)$ for some $\tau>0$; then we have

$$-\omega_0{}^2-i\omega_0\left(G-ay_*e^{-i\omega_0\tau_1}+cax_*-m\right)-mG+may_*e^{-i\omega_0\tau_1}+cax_*G=0. \tag{36}$$

Then

$$-\omega_0{}^2-i\omega_0\left(G-De^{-i\omega_0\tau_1}+F-m\right)-mG+Ee^{-i\omega_0\tau_1}+FG=0. \tag{37}$$

Where $D=ay_*$, $E=may_*$, $F=cax_*$ we know

$$e^{-i\omega_0\tau}=\cos\omega_0\tau-i\sin\omega_0\tau. \tag{38}$$

So we get

$$-\omega_0{}^2-i\omega_0G+i\omega_0D\cos\omega_0\tau_1+\omega_0D\sin\omega_0\tau_1-i\omega_0F+i\omega_0m-mG+E\cos\omega_0\tau_1-iE\sin\omega_0\tau_1+FG=0. \tag{39}$$

Separate real and imaginary parts

$$\begin{gathered}-\omega_0{}^2+\omega_0D\sin\omega_0\tau_1-mG+E\cos\omega_0\tau_1+FG=0\\ -\omega_0G+\omega_0D\cos\omega_0\tau_1-\omega_0F+\omega_0m-E\sin\omega_0\tau_1=0\end{gathered} \tag{40}$$

Then

$$\begin{gathered}\omega_0D\sin\omega_0\tau_1+E\cos\omega_0\tau_1=\omega_0{}^2-FG+mG\\ \omega_0D\cos\omega_0\tau_1-E\sin\omega_0\tau_1=\omega_0G+\omega_0F-\omega_0m\end{gathered} \tag{41}$$

So

$$\omega_0{}^4+\left(4FG-2Fm+G^2+F^2+m^2-D^2\right)\omega_0{}^2-2FmG^2+F^2G^2+m^2G^2-E^2=0 \tag{42}$$

We assume that

$$\begin{gathered}W=\omega_0{}^2\\ W^2+\left(4FG-2Fm+G^2+F^2+m^2-D^2\right)W-2FmG^2+F^2G^2+m^2G^2-E^2=0.\end{gathered} \tag{43}$$

If $4FG-2Fm+G^2+F^2+m^2-D^2>0$ and $-2FmG^2+F^2G^2+m^2G^2-E^2>0$, then all roots of equation have negative real parts for all $\tau_1>0,\tau_2=0$; that is, the equilibrium $E_*=(x_*,y_*)$ is locally asymptotically stable:

$$W=\frac{-M\pm\sqrt{M^2-4\left(-2FmG^2+F^2G^2+m^2G^2-E^2\right)}}{2} \tag{44}$$

where

$$M=4FG-2Fm+G^2+F^2+m^2-D^2. \tag{45}$$

If $-M>0, M^2=4(2FmG^2+F^2G^2+m^2G^2-E^2)$ and $-2FmG^2+F^2G^2+m^2G^2-E^2>0$, there is a unique positive solution; the equilibrium $E_*=(x_*,y_*)$ is unstable. Also if $-M>0$, $M^2>4(-2FmG^2+F^2G^2+m^2G^2-E^2)$, and $-2FmG^2+F^2G^2+m^2G^2-E^2>0$, then there are two positive solutions. We have

$$-\omega_0{}^2+\omega_0D\sin\omega_0\tau_1-mG+E\cos\omega_0\tau_1+FG=0 \tag{46}$$

So

$$\sin\omega_0\tau_1=\frac{\omega_0{}^2+mG-E\cos\omega_0\tau_1-FG}{\omega_0D} \tag{47}$$

Then, we get

$$\cos\omega_0\tau_1=\frac{EGm-EFG-\omega_0{}^2mD+\omega_0{}^2FD+\omega_0{}^2GD+\omega_0{}^2E}{\omega_0{}^2D^2+E^2}. \tag{48}$$

It shows that if $-M>0$ and $-2FmG^2+F^2G^2+m^2G^2-E^2>0$,

$$\lambda^2-\left(G-ay_*e^{-\lambda\tau_1}+cax_*+m\right)\lambda+mG-may_*e^{-\lambda\tau_1}+cax_*G=0 \tag{49}$$

has a pair of imaginary eigenvalues $\lambda=\pm i\omega_0,\eta(\overline{\tau}_1)=0$

when $\overline{\tau}_{1j}{}^{\pm}=(1/\omega_0{}^{\pm})\arccos((EGm-EFG-\omega_0{}^2mD+\omega_0{}^2FD+\omega_0{}^2GD+\omega_0{}^2E)/(\omega_0{}^2D^2+E^2))+2\pi j/\omega_0{}^{\pm}$, $j=0,1,2,\cdots$.

Next verify the cross-sectional conditions:

$$\left(\frac{d\mathrm{Re}\,(\lambda)}{d\tau_1}\right)^{-1}\neq 0 \tag{50}$$

According to

$$\lambda^2-\left(G-ay_*e^{-\lambda\tau_1}+cax_*-m\right)\lambda-mG+may_*e^{-\lambda\tau_1}+cax_*G=0 \tag{51}$$

At this time, $\tau_1=\overline{\tau}_1$, where $\overline{\tau}_1$ is the value of $\overline{\tau}_{1j}$ at $j=0$. We get

$$2\lambda\frac{d\lambda}{d\tau_1}-\frac{d\lambda}{d\tau_1}\left(G-De^{-\lambda\tau_1}+F-m\right)+\lambda De^{-\lambda\tau_1}\left(-\tau_1\frac{d\lambda}{d\tau_1}-\lambda\right)+Ee^{-\lambda\tau_1}\left(-\tau_1\frac{d\lambda}{d\tau_1}-\lambda\right)=0 \tag{52}$$

Then

$$\left(\frac{d\lambda}{d\tau_1}\right)^{-1} = -\frac{\tau_1}{\lambda} + \frac{D}{\lambda(E+\lambda D)} + \frac{[2\lambda-(G+F-m)]}{\lambda[\lambda^2-\lambda(G+F-m)-mG+FG]}.$$

$$\left(\frac{d\mathrm{Re}(\lambda)}{d\tau_1}\right)^{-1} = -\frac{D^2}{{\omega_0}^2D^2+E^2} + \frac{-(G+F-m)^2+2\left(-mG+FG-{\omega_0}^2\right)}{(G+F-m)^2{\omega_0}^2+\left(-mG+FG-{\omega_0}^2\right)^2} \neq 0. \tag{53}$$

□

Theorem 6. *Assume $A < {x_*}^2/(K-2x_*)$, when $\tau_1 = 0, \tau_2 > 0$; we have the following conclusions. (1) If $-2EmG - F^2G^2 + m^2G^2 + E^2 > 0$, the positive equilibrium $E_* = (x_*, y_*)$ is locally asymptotically stable. (2) When $-2EmG - F^2G^2 + m^2G^2 + E^2 < 0$, if $\tau_2 < \overline{\tau}_2$, the positive equilibrium $E_* = (x_*, y_*)$ is locally asymptotically stable; if $\tau_2 > \overline{\tau}_2$, the positive equilibrium is unstable. (3) Hopf bifurcation occurs when τ_2 passes the critical value*

$$\overline{\tau}_2 = \frac{1}{\omega_0}\arccos\frac{{\omega_0}^2(-m-D)F+FG(E-mG)}{-{\omega_0}^2F^2-E^2}. \tag{54}$$

Proof. The characteristic equation is

$$\lambda^2 - \left(G - ay_* + cax_*e^{-\lambda\tau_2} + m\right)\lambda + mG - may_* + cax_*e^{-\lambda\tau_2}G = 0 \tag{55}$$

Next we suppose that $\lambda(\tau_0) = i\omega_0$ is a solution of $H(\lambda)$ for some $\tau > 0$; then we have

$$-{\omega_0}^2 - i\omega_0\left(G - ay_* + cax_*e^{-i\omega_0\tau_2} - m\right) - mG + may_* + cax_*Ge^{-i\omega_0\tau_2} = 0. \tag{56}$$

Then

$$-{\omega_0}^2 - i\omega_0\left(G - D + Fe^{-i\omega_0\tau_2} - m\right) - mG + E + FGe^{-i\omega_0\tau_2} = 0. \tag{57}$$

Where $D = ay_*$, $E = may_*$, $F = cax_*$ we know

$$e^{-i\omega_0\tau} = \cos\omega_0\tau - i\sin\omega_0\tau. \tag{58}$$

So we get

$$-{\omega_0}^2 - i\omega_0G + i\omega_0D - \omega_0F\sin\omega_0\tau_2 - i\omega_0F\cos\omega_0\tau_2 + i\omega_0m - mG + E - iFG\sin\omega_0\tau_2 + FG\cos\omega_0\tau_2 = 0. \tag{59}$$

Separate real and imaginary parts

$$\begin{aligned} &-{\omega_0}^2 - \omega_0F\sin\omega_0\tau_2 - mG + E + FG\cos\omega_0\tau_2 = 0 \\ &-\omega_0G + \omega_0D - \omega_0F\cos\omega_0\tau_2 + \omega_0m - FG\sin\omega_0\tau_2 = 0 \end{aligned} \tag{60}$$

Then

$$\begin{aligned} -\omega_0F\sin\omega_0\tau_2 + FG\cos\omega_0\tau_2 &= {\omega_0}^2 - E + mG \\ -\omega_0F\cos\omega_0\tau_2 - FG\sin\omega_0\tau_2 &= \omega_0G - \omega_0D - \omega_0m \end{aligned} \tag{61}$$

So

$${\omega_0}^4 + \left(-2E - 2DG + 2Dm + G^2 - F^2 + m^2 + D^2\right){\omega_0}^2 - 2EmG - F^2G^2 + m^2G^2 + E^2 = 0 \tag{62}$$

We assume that

$$W = {\omega_0}^2$$

$$W^2 + \left(-2E - 2DG + 2Dm + G^2 - F^2 + m^2 + D^2\right)W - 2EmG - F^2G^2 + m^2G^2 + E^2 = 0 \tag{63}$$

We can easily find

$$-2E - 2DG + 2Dm + G^2 - F^2 + m^2 + D^2 > 0. \tag{64}$$

If $-2EmG - F^2G^2 + m^2G^2 + E^2 > 0$, the positive equilibrium $E_* = (x_*, y_*)$ is locally asymptotically stable,$-2EmG - F^2G^2 + m^2G^2 + E^2 < 0$, and the positive equilibrium is unstable. We have

$$-\omega_0F\sin\omega_0\tau_2 + FG\cos\omega_0\tau_2 = {\omega_0}^2 - E + mG \tag{65}$$

So

$$\sin\omega_0\tau_1 = \frac{{\omega_0}^2 - E + mG - FG\cos\omega_0\tau_2}{-\omega_0F} \tag{66}$$

Then, we get

$$\cos\omega_0\tau_2 = \frac{{\omega_0}^2(-m-D)F - FG(-E+mG)}{-{\omega_0}^2F^2 - E^2}. \tag{67}$$

It shows that if$-2EmG - F^2G^2 + m^2G^2 + E^2 < 0$,

$$\lambda^2 - \left(G - ay_* + cax_*e^{-\lambda\tau_2} - m\right)\lambda - mG + may_* + cax_*e^{-\lambda\tau_2}G = 0 \tag{68}$$

has a pair of imaginary eigenvalues $\lambda = \pm i\omega_0$, $\eta(\overline{\tau}_2) = 0$ when ${\overline{\tau}_{2j}}^{\pm} = (1/{\omega_0}^{\pm})\arccos(({\omega_0}^2(-m-D)F + FG(E-mG))/(-{\omega_0}^2F^2 - E^2)) + 2\pi j/{\omega_0}^{\pm}$, $j = 0, 1, 2, \cdots$.

Next verify the cross-sectional conditions:

$$\left(\frac{d\mathrm{Re}(\lambda)}{d\tau_2}\right)^{-1} \neq 0 \tag{69}$$

According to

$$\lambda^2-\left(G-ay_*+cax_*e^{-\lambda\tau_2}-m\right)\lambda-mG+may_* \\ +cax_*e^{-\lambda\tau_2}G=0 \quad (70)$$

At this time, $\tau_2=\overline{\tau}_2$, where $\overline{\tau}_2$ is the value of $\overline{\tau}_{2j}$ at $j=0$. We get

$$2\lambda\frac{d\lambda}{d\tau_2}-\frac{d\lambda}{d\tau_2}\left(G-D+Fe^{-\lambda\tau_2}-m\right) \\ -\lambda Fe^{-\lambda\tau_2}\left(-\tau_2\frac{d\lambda}{d\tau_2}-\lambda\right) \\ +FGe^{-\lambda\tau_2}\left(-\tau_2\frac{d\lambda}{d\tau_2}-\lambda\right)=0 \quad (71)$$

Then

$$\left(\frac{d\lambda}{d\tau_2}\right)^{-1} \\ =-\frac{\tau_2}{\lambda}-\frac{F}{\lambda(G-\lambda)} \\ +\frac{2\lambda-(G-D-m)}{\lambda\left[\lambda^2-\lambda(G-D-m)-mG+E\right]} \\ \left(\frac{d\mathrm{Re}(\lambda)}{d\tau_2}\right)^{-1} \\ =-\frac{F}{\omega_0{}^2+G^2} \\ +\frac{2\left[(-mG+E)-\omega_0{}^2\right]-(G-D-m)^2}{\omega_0{}^2(G-D-m)^2+\left[(-mG+E)-\omega_0{}^2\right]^2} \\ \neq 0. \quad (72)$$

□

Theorem 7. *Assume $A<x_*{}^2/(K-2x_*)$, when $\tau_1\neq 0,\tau_2\neq 0$; we have the following conclusions. (1) When and $G^2-F^2+m^2-D^2+2DF>0$ and $-2EFG-F^2G^2+m^2G^2-E^2>0$, the positive equilibrium $E_*=(x_*,y_*)$ is locally asymptotically stable. (2) Hopf bifurcation occurs when τ_1 passes the critical value*

$$\overline{\tau}=\frac{1}{\omega_0} \\ \cdot\arctan\frac{\left(\omega_0{}^2+mG\right)\left(\omega_0D-\omega_0F\right)-\omega_0(G-m)}{-\left(\omega_0{}^2+mG\right)(FG+E)+\omega_0(G-m)}. \quad (73)$$

Proof. The characteristic equation is

$$\lambda^2-\left(G-ay_*e^{-\lambda\tau_1}+cax_*e^{-\lambda\tau_2}-m\right)\lambda-mG \\ +may_*e^{-\lambda\tau_1}+cax_*e^{-\lambda\tau_2}G=0. \quad (74)$$

Next we suppose that $\lambda(\tau_0)=i\omega_0$ is a solution of $H(\lambda)$ for some $\tau>0$; then we have

$$-\omega_0{}^2-i\omega_0\left(G-De^{-i\omega_0\tau_1}+Fe^{-i\omega_0\tau_2}+m\right)-mG \\ +Ee^{-i\omega_0\tau_1}+FGe^{-i\omega_0\tau_2}=0. \quad (75)$$

Where $D=ay_*$, $E=may_*$, $F=cax_*$ we know

$$e^{-i\omega_0\tau}=\cos\omega_0\tau-i\sin\omega_0\tau. \quad (76)$$

So we get

$$-\omega_0{}^2-i\omega_0G+i\omega_0D\cos\omega_0\tau_1+\omega_0D\sin\omega_0\tau_1 \\ -\omega_0F\sin\omega_0\tau_2-i\omega_0F\cos\omega_0\tau_2+i\omega_0m-mG \\ +E\cos\omega_0\tau_1-iE\sin\omega_0\tau_1-iFG\sin\omega_0\tau_2 \\ +FG\cos\omega_0\tau_2=0 \quad (77)$$

Separate real and imaginary parts

$$-\omega_0{}^2+\omega_0D\sin\omega_0\tau_1-\omega_0F\sin\omega_0\tau_2-mG \\ +E\cos\omega_0\tau_1+FG\cos\omega_0\tau_2=0 \\ -\omega_0G+\omega_0D\cos\omega_0\tau_1-\omega_0F\cos\omega_0\tau_2+\omega_0m \\ -FG\sin\omega_0\tau_2-E\sin\omega_0\tau_1=0 \quad (78)$$

Let $\tau_1=\tau_2=\tau>0$. Then

$$\omega_0D\sin\omega_0\tau-\omega_0F\sin\omega_0\tau+E\cos\omega_0\tau \\ +FG\cos\omega_0\tau=\omega_0{}^2+mG \\ \omega_0D\cos\omega_0\tau-\omega_0F\cos\omega_0\tau-FG\sin\omega_0\tau \\ -E\sin\omega_0\tau=\omega_0G-\omega_0m \quad (79)$$

So

$$\omega_0{}^4+\left(G^2-F^2+m^2-D^2+2DF\right)\omega_0{}^2-2EFH \\ -F^2G^2+m^2G^2-E^2=0 \quad (80)$$

We assume that

$$W=\omega_0{}^2 \\ W^2+\left(G^2-F^2+m^2-D^2+2DF\right)W-2EFH \\ -F^2G^2+m^2G^2-E^2=0 \quad (81)$$

If $G^2-F^2+m^2-D^2+2DF>0$ and $-2EFH-F^2G^2+m^2G^2-E^2>0$, then all roots of equation have negative real parts for all $\tau_1>0,\tau_2>0$; that is, the equilibrium $E_*=(x_*,y_*)$ is locally asymptotically stable:

$$W=\frac{-N\pm\sqrt{N^2-4\left(-2EFH-F^2G^2+m^2G^2-E^2\right)}}{2} \quad (82)$$

where

$$N = G^2 - F^2 + m^2 - D^2 + 2DF \quad (83)$$

If $-N > 0$, $N^2 = 4(-2EFH - F^2G^2 + m^2G^2 - E^2)$, and $-2EFH - F^2G^2 + m^2G^2 - E^2 > 0$, there is a unique positive solution; the equilibrium $E_* = (x_*, y_*)$ is unstable. Also if $-N > 0$, $N^2 > 4(-2EFH - F^2G^2 + m^2G^2 - E^2)$, and $-2EFH - F^2G^2 + m^2G^2 - E^2 > 0$, then there are two positive solutions. We have

$$\begin{aligned} &\omega_0 D \sin \omega_0 \tau - \omega_0 F \sin \omega_0 \tau + E \cos \omega_0 \tau \\ &\quad + FG \cos \omega_0 \tau = \omega_0{}^2 + mG \\ &\omega_0 D \cos \omega_0 \tau - \omega_0 F \cos \omega_0 \tau - FG \sin \omega_0 \tau \\ &\quad - E \sin \omega_0 \tau = \omega_0 G - \omega_0 m \end{aligned} \quad (84)$$

So

$$\begin{aligned} \sin \omega_0 \tau &= \frac{\left(\omega_0{}^2 + mG\right)\left(\omega_0 D - \omega_0 F\right) - \omega_0 (G - m)}{\left(\omega_0 D - \omega_0 F\right)^2 - (FG + E)^2} \\ \cos \omega_0 \tau &= \frac{-\left(\omega_0{}^2 + mG\right)(FG + E) + \omega_0 (G - m)}{\left(\omega_0 D - \omega_0 F\right)^2 - (FG + E)^2} \end{aligned} \quad (85)$$

Then, we get

$$\tan \omega_0 \tau = \frac{\left(\omega_0{}^2 + mG\right)\left(\omega_0 D - \omega_0 F\right) - \omega_0 (G - m)}{-\left(\omega_0{}^2 - mG\right)(FG + E) + \omega_0 (G - m)}. \quad (86)$$

It shows that if $-2EFH - F^2G^2 + m^2G^2 - E^2 < 0$,

$$\begin{aligned} &\lambda^2 - \left(G - a y_* e^{-\lambda \tau_1} + c a x_* e^{-\lambda \tau_2} - m\right) \lambda - mG \\ &\quad + m a y_* e^{-\lambda \tau_1} + c a x_* e^{-\lambda \tau_2} G = 0 \end{aligned} \quad (87)$$

has a pair of imaginary eigenvalues $\lambda = \pm i\omega_0$, $\eta(\overline{\tau}_1) = 0$ when $\overline{\tau}_j{}^{\pm} = (1/\omega_0{}^{\pm}) \arctan(((\omega_0{}^2 + mG)(\omega_0{}^{\pm} D - \omega_0{}^{\pm} F) - \omega_0{}^{\pm}(G - m))/(-(\omega_0{}^2 + mG)(FG + E) + \omega_0{}^{\pm}(G - m))) + \pi j/\omega_0{}^{\pm}$, $j = 0, 1, 2, \cdots$.

Next verify the cross-sectional conditions:

$$\left(\frac{d\mathrm{Re}(\lambda)}{d\tau}\right)^{-1} \neq 0 \quad (88)$$

According to

$$\begin{aligned} &\lambda^2 - \left(G - a y_* e^{-\lambda \tau_1} + c a x_* e^{-\lambda \tau_2} - m\right) \lambda - mG \\ &\quad + m a y_* e^{-\lambda \tau_1} + c a x_* e^{-\lambda \tau_2} G = 0 \end{aligned} \quad (89)$$

At this time,$\tau = \overline{\tau}$, where $\overline{\tau}$ is the value of $\overline{\tau}_j$ at $j = 0$. We get

$$\begin{aligned} &2\lambda \frac{d\lambda}{d\tau} - \frac{d\lambda}{d\tau}\left(G - De^{-\lambda\tau} + Fe^{-\lambda\tau} - m\right) \\ &\quad + \lambda De^{-\lambda\tau}\left(-\tau \frac{d\lambda}{d\tau} - \lambda\right)\lambda \\ &\quad - \lambda Fe^{-\lambda\tau}\left(-\tau \frac{d\lambda}{d\tau} - \lambda\right) + Ee^{-\lambda\tau}\left(-\tau \frac{d\lambda}{d\tau} - \lambda\right) \\ &\quad + FGe^{-\lambda\tau}\left(-\tau \frac{d\lambda}{d\tau} - \lambda\right) = 0 \end{aligned} \quad (90)$$

Then

$$\begin{aligned} \left(\frac{d\lambda}{d\tau}\right)^{-1} &= -\frac{\tau}{\lambda} - \frac{F - D}{\lambda (\lambda D - \lambda F + E + FG)} \\ &\quad + \frac{2\lambda - (G - m)}{\lambda \left[\lambda^2 - \lambda (G - m) - mG\right]} \\ \left(\frac{d\mathrm{Re}(\lambda)}{d\tau}\right)^{-1} &= \frac{-(F - D)^2}{\omega_0{}^2 (F - D)^2 + (FG + E)^2} \\ &\quad + \frac{2\left(-mG - \omega_0{}^2\right) - (G - m)^2}{\omega_0{}^2 (G - m)^2 + \left(-mG - \omega_0{}^2\right)^2} \\ &\neq 0. \end{aligned} \quad (91)$$

□

4. Numerical Simulations

In this section, we present some numerical simulations to illustrate our theoretical analysis.

First, we theoretically analyze a predator-prey model with Allee effect in the article and obtain the stability conditions of $E_1 = (K, 0)$ and $E_* = (x_*, y_*)$. Secondly, we carry out numerical simulation and select appropriate the parameters, which draw the stable positions of the equilibrium points $E_1 = (K, 0)$ and $E_* = (x_*, y_*)$, shown in Figures 1 and 2. In the analysis later in this chapter, we use A as the bifurcation parameter to obtain the critical value of the Hopf bifurcation generated by the model (2). By comparing Figures 3 and 4, we find that as the parameter A changes the equilibrium point changes from a steady state to a limit cycle. To further verify our point of view, we have made a bifurcation diagram as shown in Figure 5. We found that the bifurcation parameter produced a bifurcation at about 100, which coincided with our previous guess. By the same analysis method, we give a set of timing diagrams for comparison as shown in Figures 6 and 7; we found that with the increase of the parameter A the model (2) is shown in Figure 6 and the population gradually becomes stable with the increase of time, while Figure 7 is a periodic change.

Next, we performed a numerical simulation of the model (3), mainly to study the effect of the time-delay parameter τ on the stability of the coexistence equilibrium point. Here, we compare three sets of timing diagrams, which are the effect of τ_1 on the stability of the coexistence equilibrium point, the influence of τ_2 on the stability of the coexistence equilibrium point, and the influence of $\tau_1 = \tau_2 = \tau$ on the stability of the coexistence equilibrium point. First, by comparing Figures 8 and 9, we find that when $\tau_1 = 0.1$, the population gradually becomes stable with the increase of time. When $\tau_1 = 0.25$, the population gradually shows periodicity with the increase of time. By comparing Figures 10 and 11, we find that when $\tau_2 = 0.1$, the population gradually becomes stable with the increase of time. When $\tau_2 = 1.5$, the

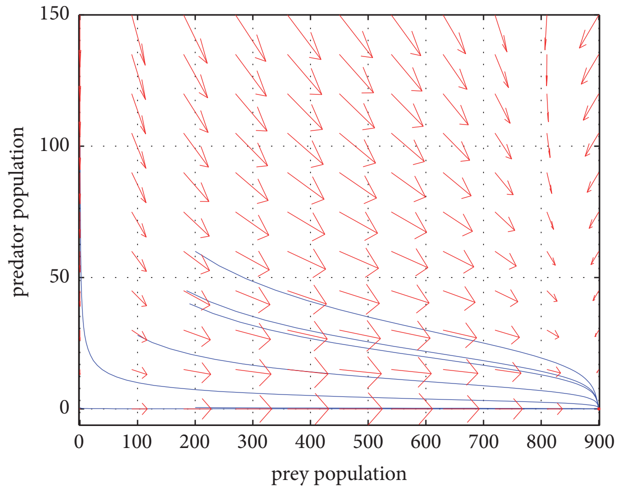

Figure 1: The phase portrait of model (2) with weak Allee effect. The parameters are taken as $A = 0.01$, $r = 2.65$, $K = 900$, $a = 0.002$, $c = 0.215$, and $m = 1.06$; $E_1 = (K, 0)$ is locally asymptotically stable.

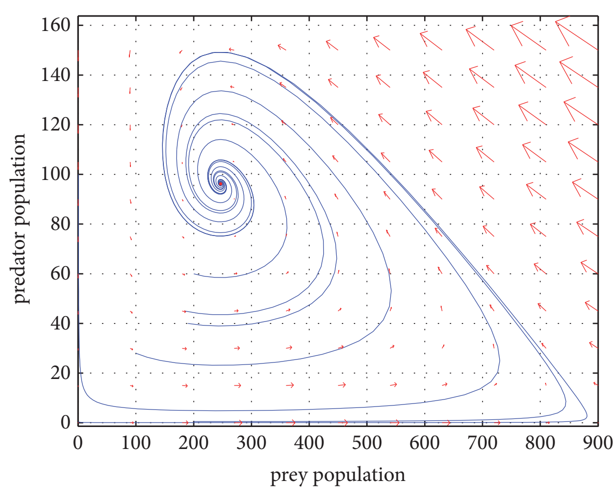

Figure 2: The phase portrait of model (2) with weak Allee effect. The parameters are taken as $A = 0.01$, $r = 2.65$, $K = 900$, $a = 0.02$, $c = 0.215$, and $m = 1.06$; $E_* = (x_*, y_*)$ is locally asymptotically stable.

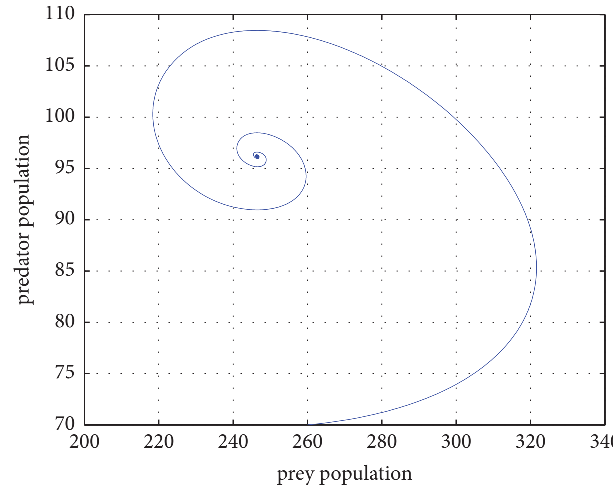

Figure 3: The phase portrait of model (2) with weak Allee effect. The parameters are taken as $x(0) = 260$, $y(0) = 70$, $A = 0.01$, $r = 2.65$, $K = 900$, $a = 0.02$, $c = 0.215$, and $m = 1.06$; $E_* = (x_*, y_*)$ is locally asymptotically stable, with no limit cycle.

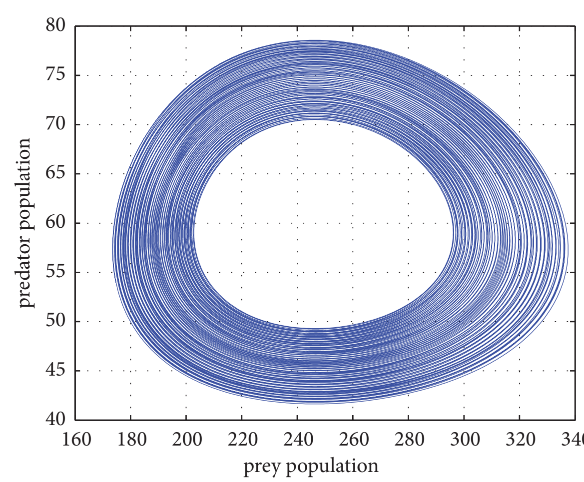

Figure 4: The phase portrait of model (2) with weak Allee effect. The parameters are taken as $x(0) = 260$, $y(0) = 70$, $A = 150$, $r = 2.65$, $K = 900$, $a = 0.02$, $c = 0.215$, and $m = 1.06$; $E_* = (x_*, y_*)$ becomes unstable; a limit cycle is formed.

population gradually shows periodicity with the increase of time; by comparing Figures 12 and 13, we found that when $\tau = 0.1$, the population gradually becomes stable with the increase of time. When $\tau = 0.19$, the population gradually shows periodicity with the increase of time. At the same time, we selected the appropriate parameters and gave three sets of phase diagrams for comparison. By comparing Figures 14 and 15, we find that when τ_1 increases from 0.1 to 0.25, the coexistence equilibrium point changes from a steady state to a limit cycle; by comparing Figures 16 and 17, we find that τ_2 is increased from 0.1 to 1.5. At this time, the coexistence equilibrium point changes from a steady state to a limit cycle; by comparing Figures 18 and 19, we find that when τ increases from 0.1 to 0.19, the coexistence equilibrium point changes from a steady state to a limit cycle. From this, we can conclude that the stability of the equilibrium point of the model (3) changes with the increase of the time lag when the time-delay parameter is introduced, and the generation of the limit cycle (periodic solution) is accompanied by this change.

5. Conclusions

In this paper, we establish a predator-prey model with a weak Allee effect and demonstrate and analyze the boundedness and stability of the model. We also prove that the model

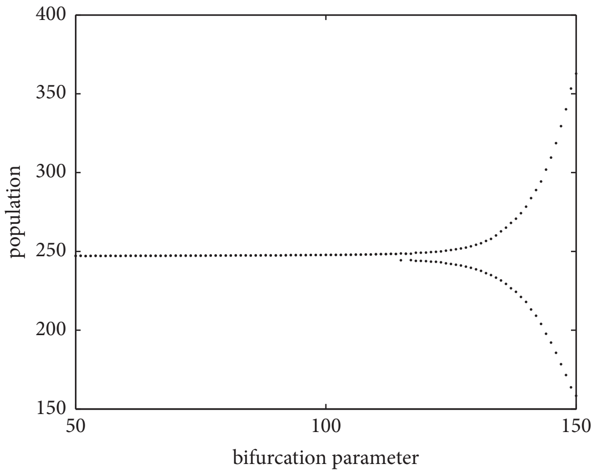

Figure 5: Bifurcation diagram with respect to the parameter A; other parameter values are $r = 2.65$, $K = 900$, $a = 0.02$, $c = 0.215$, and $m = 1.06$.

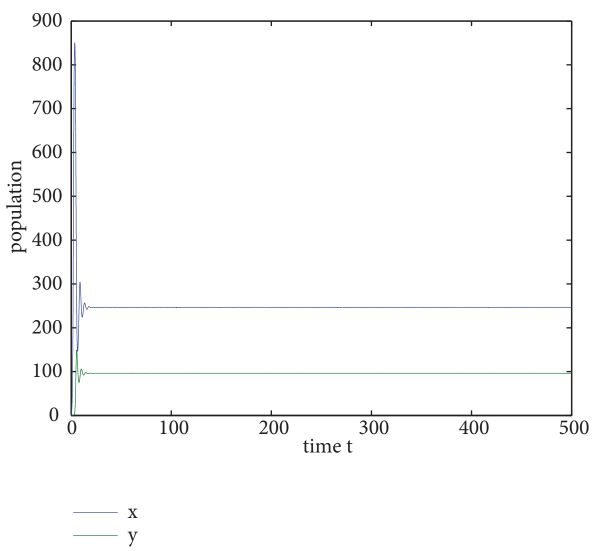

Figure 6: A Time series diagram for prey and predator. The figure depicts local stability of the interior equilibrium for the model (2), where the parameter values are $x(0) = 230$, $y(0) = 95$, $A = 0.01$, $r = 2.65$, $K = 900$, $a = 0.02$, $c = 0.215$, and $m = 1.06$.

(2) experiences transcritical bifurcation around the axial equilibrium and the model (2) undergoes a Hopf bifurcation at $E_* = (x_*, y_*)$ when $A = A_0$; we also analyzed the direction and stability of Hopf bifurcation. Immediately after we introduced the searching delay and digestion delay in the model (2), a new model was obtained, and the model (3) was analyzed for stability changes caused by time lag. It is concluded that the stability of the coexistence equilibrium point of the model (3) changes as the time lag increases. Finally, we verify our theoretical derivation by numerical simulation. First, we select the appropriate parameters to

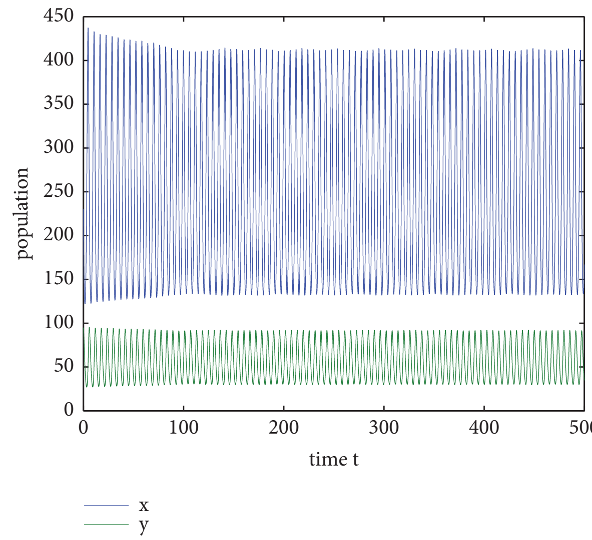

Figure 7: A Time series diagram for prey and predator. Existence of periodic solution around the interior equilibrium $E_* = (x_*, y_*)$ for the model (2), where the parameter values are $x(0) = 230$, $y(0) = 95$, $A = 150$, $r = 2.65$, $K = 900$, $a = 0.02$, $c = 0.215$, and $m = 1.06$.

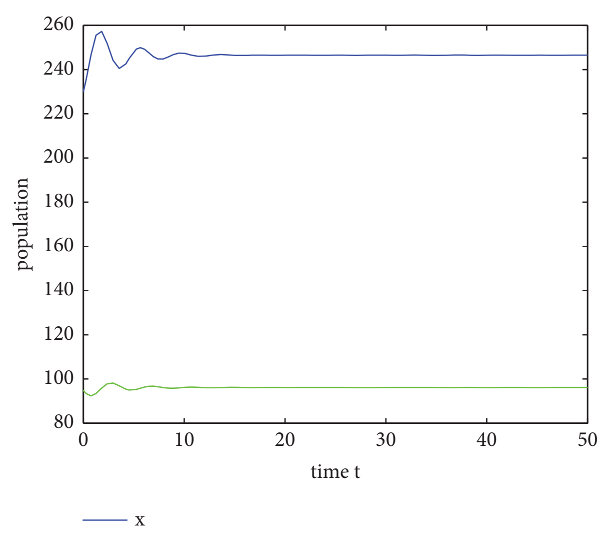

Figure 8: A Time series diagram for prey and predator. The figure depicts local stability of the interior equilibrium for the delayed model (3) with the time delays $\tau_1 = 0.1$ and $\tau_2 = 0$, where the other parameter values are $x(0) = 230$, $y(0) = 95$, $A = 0.01$, $r = 2.65$, $K = 900$, $a = 0.02$, $c = 0.215$, and $m = 1.06$.

satisfy the stable conditions that we deduced in the article and obtain the stable phase diagrams of the equilibrium points $E_1 = (K, 0)$ and $E_* = (x_*, y_*)$. Second, we try to change the value of parameter A, the timing diagram, phase diagram, and bifurcation diagram corresponding to each parameter drawn. Further verification of our conclusion is as A increases, the model (2) will produce bifurcation. We

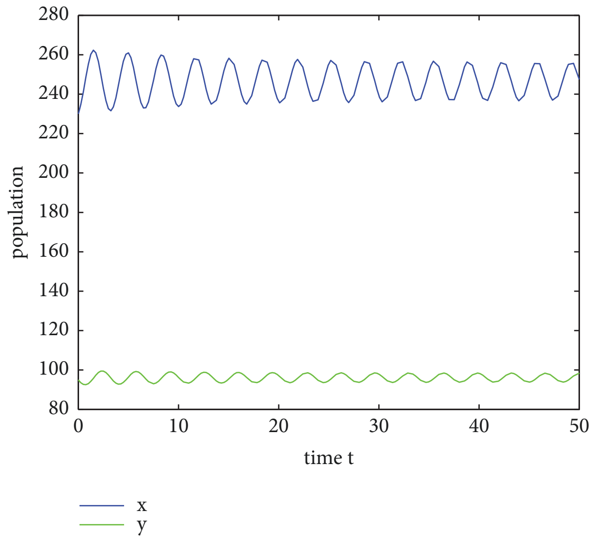

Figure 9: A Time series diagram for prey and predator. Existence of periodic solution around the interior equilibrium $E_* = (x_*, y_*)$ for delayed model (3) with the time delays $\tau_1 = 0.25$ and $\tau_2 = 0$, where the parameter values are $x(0) = 230$, $y(0) = 95$, $A = 0.01$, $r = 2.65$, $K = 900$, $a = 0.02$, $c = 0.215$, and $m = 1.06$.

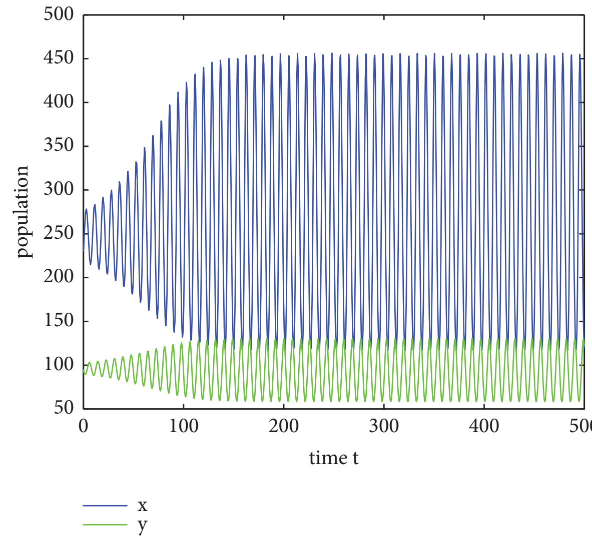

Figure 11: A Time series diagram for prey and predator. Existence of periodic solution around the interior equilibrium $E_* = (x_*, y_*)$ for delayed model (3) with the time delays $\tau_1 = 0$ and $\tau_2 = 1.5$, where the parameter values are $x(0) = 230$, $y(0) = 95$, $A = 0.01$, $r = 2.65$, $K = 900$, $a = 0.02$, $c = 0.215$, and $m = 1.06$.

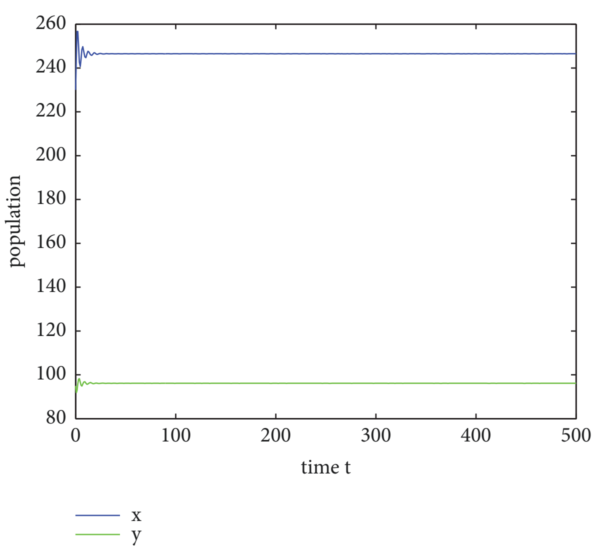

Figure 10: A Time series diagram for prey and predator. The figure depicts local stability of the interior equilibrium for the delayed model (3) with the time delays $\tau_1 = 0$ and $\tau_2 = 0.1$, where the other parameter values are $x(0) = 230$, $y(0) = 95$, $A = 0.01$, $r = 2.65$, $K = 900$, $a = 0.02$, $c = 0.215$, and $m = 1.06$.

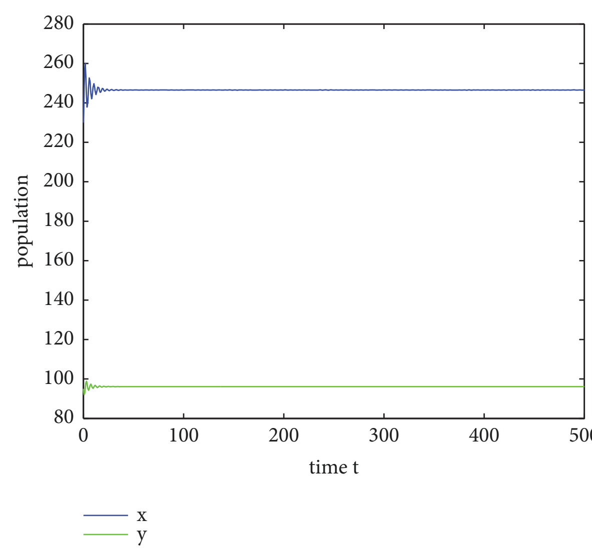

Figure 12: A Time series diagram for prey and predator. The figure depicts local stability of the interior equilibrium for the delayed model (3) with the time delay $\tau_1 = \tau_2 = 0.1$, where the other parameter values are $x(0) = 230$, $y(0) = 95$, $A = 0.01$, $r = 2.65$, $K = 900$, $a = 0.02$, $c = 0.215$, and $m = 1.06$.

also carry out a numerical model of the model (3) and discuss our numerical results in three groups: at the beginning, let τ_1 change, $\tau_2 = 0$; we observe the timing diagram corresponding to the model (3) as τ_1 increases. In the change of the phase diagram, we find that with the increase of τ_1 the coexistence equilibrium point of the model (3) begins to stabilize and becomes unstable and is also accompanied by the generation of the limit cycle (periodic solution); we also change the τ_2, $\tau_1 = 0$; we observe the increase of τ_2, corresponding to the change of the phase diagram of the time series of the model (3); we find that with the increase of τ_2 the coexistence equilibrium point of the model (3) begins to stabilize and

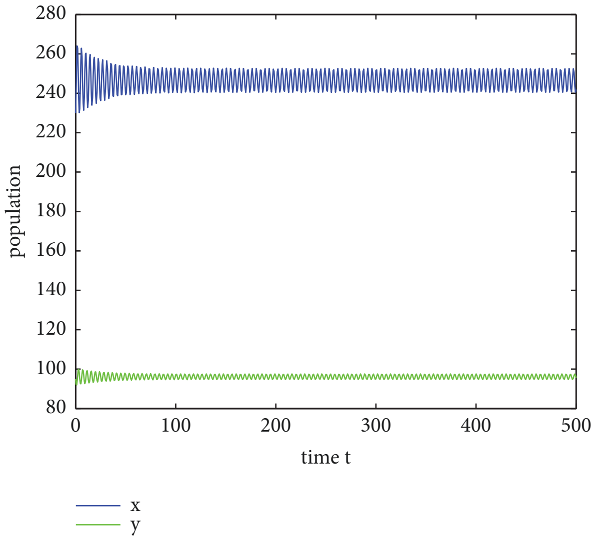

FIGURE 13: A Time series diagram for prey and predator. Existence of periodic solution around the interior equilibrium $E_* = (x_*, y_*)$ for delayed model (3) with the time delay $\tau_1 = \tau_2 = 0.19$, where the parameter values are $x(0) = 230$, $y(0) = 95$, $A = 0.01$, $r = 2.65$, $K = 900$, $a = 0.02$, $c = 0.215$, and $m = 1.06$.

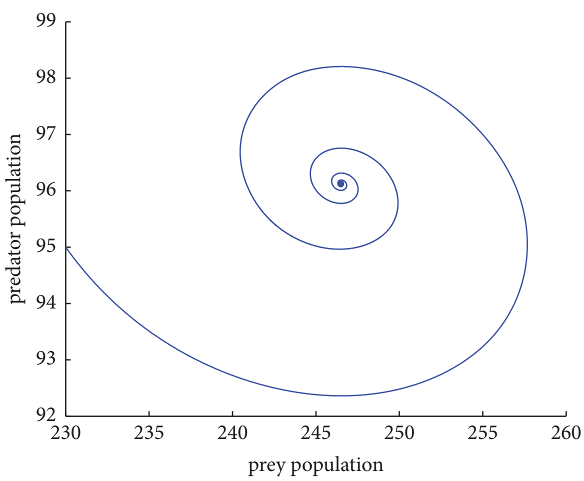

FIGURE 14: The phase portrait of delayed model (3) with the time delays $\tau_1 = 0.1$ and $\tau_2 = 0$. The parameters are taken as $x(0) = 230$, $y(0) = 95$, $A = 0.01$, $r = 2.65$, $K = 900$, $a = 0.02$, $c = 0.215$, and $m = 1.06$; $E_* = (x_*, y_*)$ is locally asymptotically stable, with no limit cycle.

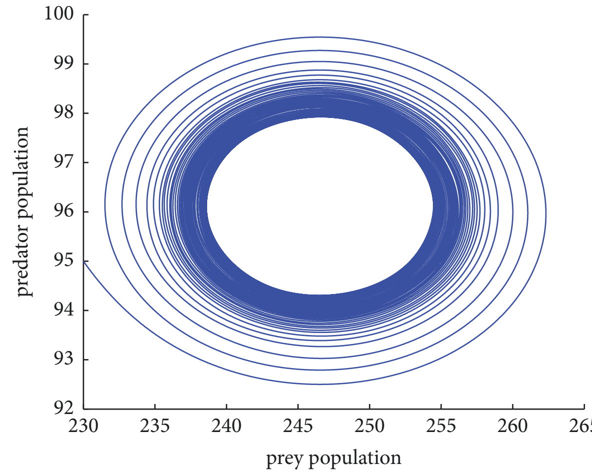

FIGURE 15: The phase portrait of delayed model (3) with the time delays $\tau_1 = 0.25$ and $\tau_2 = 0$. The parameters are taken as $x(0) = 230$, $y(0) = 95$, $A = 0.01$, $r = 2.65$, $K = 900$, $a = 0.02$, $c = 0.215$, and $m = 1.06$; $E_* = (x_*, y_*)$ becomes unstable; a limit cycle is formed.

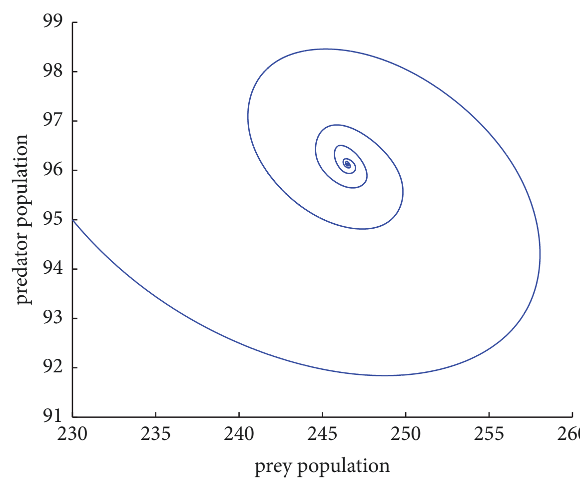

FIGURE 16: The phase portrait of delayed model (3) with the time delays $\tau_1 = 0$ and $\tau_2 = 0.1$. The parameters are taken as $x(0) = 230, y(0) = 95, A = 0.01, r = 2.65, K = 900, a = 0.02, c = 0.215$, and $m = 1.06$; $E_* = (x_*, y_*)$ is locally asymptotically stable, with no limit cycle.

becomes unstable. At the same time, it is accompanied by the generation of the limit cycle (periodic solution); the same we let $\tau_1 = \tau_2 = \tau$, so that τ increases; we also found similar changes. In this process, we also found an interesting phenomenon. When τ_1 takes a small value, the stability of the coexistence equilibrium point of the model changes. However, τ_2 requires a larger value than τ_1. When $\tau_1 = \tau_2 = \tau$, τ only needs to take a small value, and the stability of the coexistence equilibrium point of the model changes. From a biological point of view, we find that the introduction of weak Allee effect will change the stability of the model; that is to say, the stable state between populations will be broken. Similarly, delays can destroy the stability of the original predator-prey model. Moreover, the introduction of delay and weak Allee effect makes the model closer to reality and makes us more accurately understand the dynamic changes of interspecific relationships. Therefore, we can find that Allee effect and delay play an important role in describing population dynamics.

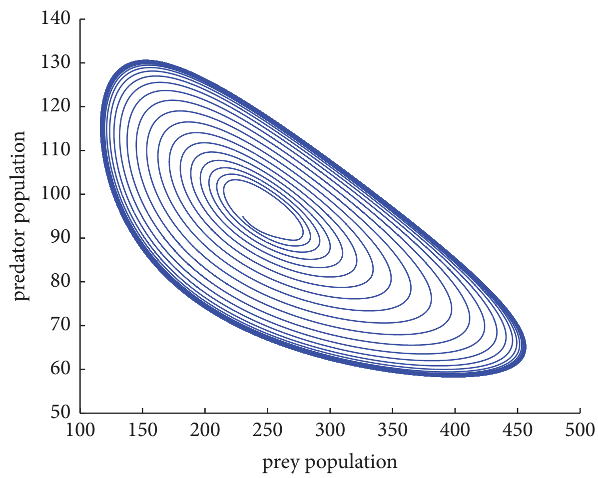

Figure 17: The phase portrait of delayed model (3) with the time delays $\tau_1 = 0$ and $\tau_2 = 1.5$. The parameters are taken as $x(0) = 230$, $y(0) = 95$, $A = 0.01$, $r = 2.65$, $K = 900$, $a = 0.02$, $c = 0.215$, and $m = 1.06$; $E_* = (x_*, y_*)$ becomes unstable; a limit cycle is formed.

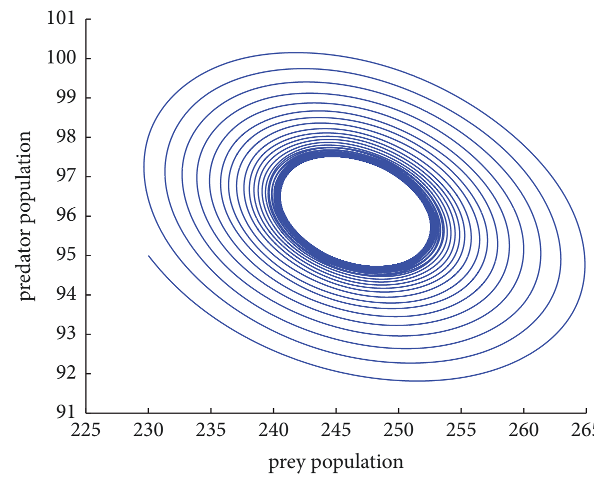

Figure 19: The phase portrait of delayed model (3) with the time delay $\tau_1 = \tau_2 = 0.19$. The parameters are taken as $x(0) = 230$, $y(0) = 95$, $A = 0.01$, $r = 2.65$, $K = 900$, $a = 0.02$, $c = 0.215$, and $m = 1.06$; $E_* = (x_*, y_*)$ becomes unstable; a limit cycle is formed.

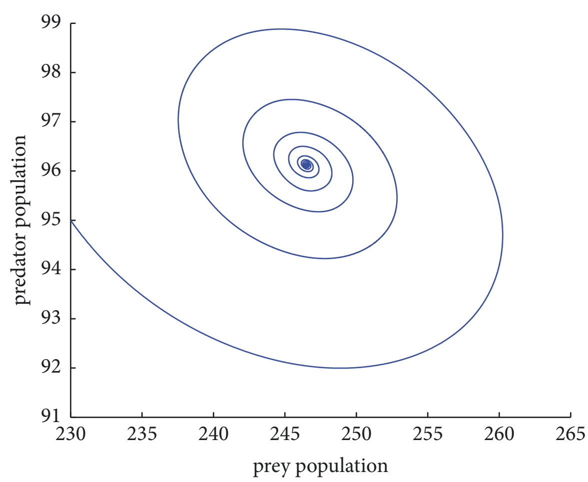

Figure 18: The phase portrait of delayed model (3) with the time delay $\tau_1 = \tau_2 = 0.1$. The parameters are taken as $x(0) = 230$, $y(0) = 95$, $A = 0.01$, $r = 2.65$, $K = 900$, $a = 0.02$, $c = 0.215$, and $m = 1.06$; $E_* = (x_*, y_*)$ is locally asymptotically stable, with no limit cycle.

Data Availability

The data used to support the findings of this study are included within the article.

Conflicts of Interest

The authors declare that they have no conflicts of interest.

Acknowledgments

This work was supported by the National Natural Science Foundation of China (31260098, 31560127), the Fundamental Research Funds for the Central Universities (31920180116, 31920180044, and 31920170072), the Program for Yong Talent of State Ethnic Affairs Commission of China (No. [2014]121), Gansu Provincial First-Class Discipline Program of Northwest Minzu University, and Central Universities Fundamental Research Funds for the Graduate Students of Northwest Minzu University (Yxm2019109).

References

[1] V. Volterra, "Fluctuations in the abundance of a species considered mathematically," *Nature*, vol. 118, no. 2972, pp. 558–560, 1926.

[2] A. J. Lotka, *Elements of Physical Biology*, Williams and Wilkins, Pennsylvania, Pa, USA, 1926.

[3] F. Courchamp, T. Clutton-Brock, and B. Grenfell, "Inverse density dependence and the Allee effect," *Trends in Ecology & Evolution*, vol. 14, no. 10, pp. 405–410, 1999.

[4] P. A. Stephens, W. J. Sutherland, and R. P. Freckleton, "What is the allee effect?" *Oikos*, vol. 87, no. 1, pp. 185–190, 1999.

[5] P. A. Stephens and W. J. Sutherland, "Consequences of the allee effect for behaviour, ecology and conservation," *Trends in Ecology & Evolution*, vol. 14, no. 10, pp. 401–405, 1999.

[6] W. C. Allee, *Animal Aggregations: A study in General Sociology*, University of Chicago Press, Illinois, Ill, USA, 1931.

[7] A. Deredec and F. Courchamp, "Extinction thresholds in host-parasite dynamics," *Annales Zoologici Fennici*, vol. 40, no. 2, pp. 115–130, 2003.

[8] M.-H. Wang and M. Kot, "Speeds of invasion in a model with strong or weak Allee effects," *Mathematical Biosciences*, vol. 171, no. 1, pp. 83–97, 2001.

[9] C. W. Fowler and J. D. Baker, "A review of animal population dynamics at extremely reduced population levels," *Report - International Whaling Commission*, vol. 41, pp. 545–554, 1991.

[10] S. J. Schreiber, "Allee effects, extinctions, and chaotic transients in simple population models," *Theoretical Population Biology*, vol. 64, no. 2, pp. 201–209, 2003.

[11] M. Wang, M. Kot, and M. G. Neubert, "Integrodifference equations, Allee effects, and invasions," *Journal of Mathematical Biology*, vol. 44, no. 2, pp. 150–168, 2002.

[12] G. Wang, X.-G. Liang, and F.-Z. Wang, "The competitive dynamics of populations subject to an Allee effect," *Ecological Modelling*, vol. 124, no. 2-3, pp. 183–192, 1999.

[13] R. Lin, S. Liu, and X. Lai, "Bifurcations of a predator-prey system with weak allee effects," *Journal of the Korean Mathematical Society*, vol. 50, no. 4, pp. 695–713, 2013.

[14] S.-R. Zhou, Y.-F. Liu, and G. Wang, "The stability of predator-prey systems subject to the Allee effects," *Theoretical Population Biology*, vol. 67, no. 1, pp. 23–31, 2005.

[15] L. Shi, H. Liu, Y. Wei, M. Ma, and J. Ye, "The permanence and periodic solution of a competitive system with infinite delay, feedback control, and Allee effect," *Advances in Difference Equations*, vol. 2018, no. 1, article 400, 2018.

[16] H. Liu, Z. Li, M. Gao, H. Dai, and Z. Liu, "Dynamics of a host-parasitoid model with Allee effect for the host and parasitoid aggregation," *Ecological Complexity*, vol. 6, no. 3, pp. 337–345, 2009.

[17] J. Wang, J. Shi, and J. Wei, "Predator-prey system with strong Allee effect in prey," *Journal of Mathematical Biology*, vol. 62, no. 3, pp. 291–331, 2011.

[18] J. Wang, J. Shi, and J. Wei, "Dynamics and pattern formation in a diffusive predator-prey system with strong Allee effect in prey," *Journal of Differential Equations*, vol. 251, no. 4-5, pp. 1276–1304, 2011.

[19] Y. Cai, C. Zhao, W. Wang, and J. Wang, "Dynamics of a Leslie-Gower predator-prey model with additive Allee effect," *Applied Mathematical Modelling: Simulation and Computation for Engineering and Environmental Systems*, vol. 39, no. 7, pp. 2092–2106, 2015.

[20] C. Li and H. Zhu, "Canard cycles for predator-prey systems with holling types of functional response," *Journal of Differential Equations*, vol. 254, no. 2, pp. 879–910, 2013.

[21] Y. Li and D. Xiao, "Bifurcations of a predator-prey system of holling and leslie types," *Chaos, Solitons & Fractals*, vol. 34, no. 2, pp. 606–620, 2007.

[22] Y. Qu and J. Wei, "Bifurcation analysis in a time-delay model for prey-predator growth with stage-structure," *Nonlinear Dynamics*, vol. 49, no. 1-2, pp. 285–294, 2007.

[23] J. P. Tripathi, S. Tyagi, and S. Abbas, "Global analysis of a delayed density dependent predator-prey model with Crowley-Martin functional response," *Communications in Nonlinear Science and Numerical Simulation*, vol. 30, no. 1–3, pp. 45–69, 2016.

[24] J. Ylikarjula, S. Alaja, J. Laakso, and D. Tesar, "Effects of patch number and dispersal patterns on population dynamics and synchrony," *Journal of Theoretical Biology*, vol. 207, no. 2-3, pp. 377–387, 2000.

[25] X. Wang and J. Wei, "Dynamics in a diffusive predator-prey system with strong Allee effect and Ivlev-type functional response," *Journal of Mathematical Analysis and Applications*, vol. 422, no. 2, pp. 1447–1462, 2015.

[26] Z. Ma, H. Tang, S. Wang, and T. Wang, "Bifurcation of a predator-prey system with generation delay and habitat complexity," *Journal of the Korean Mathematical Society*, vol. 55, no. 1, pp. 43–58, 2018.